Molecular characterization of breast cancer cell lines by a low-density microarray

FRANCOISE DE LONGUEVILLE[1*], MARC LACROIX[2*], ANNA-MARIA BARBUTO[3], VINCENT BERTHOLET[1], DOMINIQUE GALLO[2], DENIS LARSIMONT[3], LAURENCE MARCQ[1], NATHALIE ZAMMATTEO[1], SOPHIE BOFFE[1], GUY LECLERCQ[2] and JOSE REMACLE[4]

[1]Eppendorf Array Technologies (EAT), 20 rue du Séminaire, 5000 Namur; [2]Laboratoire Jean-Claude Heuson de Cancérologie Mammaire; [3]Service d'Anatomie Pathologique, Institut Jules Bordet, University of Bruxelles, 127 boulevard de Waterloo, 1000 Bruxelles; [4]Laboratory of Biochemistry and Cellular Biology, University of Namur, 61 rue de Bruxelles, 5000 Namur, Belgium

Received May 3, 2005; Accepted June 20, 2005

Abstract. We designed a low-density microarray carrying 132 DNA capture sequences highly specific for genes known to be differentially expressed among breast tumors and BCC lines or associated with specific tumor properties (cell-cycle alteration, proteolysis, adhesion, hormone sensitivity, etc). We analyzed gene expression in 11 BCC lines among which 6 had already been extensively studied (BT-474, Hs578T, MCF-7, MDA-MB-231, MDA-MB-453, T-47D) and 5 were still poorly characterized (Evsa-T, IBEP-1, IBEP-2, IBEP-3, KPL-1). Some data obtained were verified or extended by real-time polymerase chain reaction (real-time PCR), Northern blotting, Western blotting, immunohistochemistry and cell growth studies. Clustering analysis of the low-density microarray data allowed the sorting of BCC lines into two classes and supported a major discriminatory role for ERα, confirming data from previous studies. A few genes that are highly and specifically expressed in one cell line were identified, such as *MGB1* (mammaglobin 1) in Evsa-T cells, and *PIP* (prolactin-inducible protein) in MDA-MB-453 BCC, suggesting an apocrine origin for these latter cells. Two BCC lines (IBEP-1 and IBEP-3) that had been previously characterized as ERα-negative, were classified by the low-density microarray among ERα-positive lines (MCF-7, T-47D, IBEP-2, BT-474, KPL-1) and were indeed confirmed as receptor-positive (at both mRNA and protein levels) and hormone-responsive cells. In conclusion, our results support the utility of a low-density microarray approach in cases where the cost and exhaustiveness of high-density microarrays may constitute a drawback; for instance, in obtaining a rapid phenotype evaluation in cell populations freshly isolated from breast tumors.

Correspondence to: Dr Françoise de Longueville, Eppendorf Array Technologies (EAT), 20a rue du Séminaire, 5000 Namur, Belgium
E-mail: delongueville.f@eppendorf.be

*Contributed equally

Abbreviations: BCC, breast cancer cell; C_T, threshold cycle; Cy3, Cyanin 3; ERα, estrogen receptor-α; HKG, housekeeping gene; MGB1, mammaglobin 1; MOPS, 3-(N-morpholino) propane sulfonic acid; mRNA, messenger RNA; PIP, prolactin-inducible protein; PMT, photomultiplier tube; Rn, normalized reporter

Key words: low-density array, breast cancer, breast cell lines (BCC lines)

Introduction

DNA microarrays allow a simultaneous, fast and standardized analysis of multiple mRNA in breast tumors and breast cancer cell (BCC) lines (reviewed in refs. 1-3). Currently, most described microarrays support thousands of DNA fragments (high-density arrays) and are designed to give the most complete view of gene expression and regulation in samples. They may also be useful for identifying previously unknown genes that are associated with the successive stages of tumor progression, with tumor responses to various therapies, or with the activation of peculiar signaling pathways.

Attempts to classify breast tumors and BCC lines by high-density microarrays led to the initially unexpected observation that they could be sorted into very few classes, based on their global gene expression profile (4,5). Regarding BCC lines, two major phenotypes were observed, based on the expression status of the estrogen receptor-α (ERα, gene *ESR1*). For instance, among the widely used BCC lines, the ERα-positive MCF-7 and T-47D cells expressed high amounts of several markers that are characteristic of the luminal breast epithelial cells. The ERα-negative MDA-MB-231 and Hs578T cells exhibited several markers generally found at a high(er) level in cells of mesenchymal origin (i.e., fibroblasts). Of interest, many of the genes composing the 'luminal epithelial-like' and 'fibroblast-like' signatures had been individually identified during the last decade as strong discriminators between the MCF-7 and/or T-47D BCC and the MDA-MB-231 and/or Hs578T BCC (for more details about molecular signatures in BCC lines, see refs. 2,4,6,7).

While high-density microarrays have been widely used in gene expression analysis, their major disadvantages are related to their high cost, the quantification reliability and time required for analysis and interpretation of the overwhelming data they provide ('non-oriented approach'). This may appear as a major drawback for some investigators and thus limit their use in numerous fields. On the contrary, low-density microarrays, consisting in a limited number of carefully selected probes to analyze gene expression, have been used for fast, reliable and cost effective investigations in various fields (8-10). We made the assumption that this tool would be useful for some targeted studies on breast cancer material. For instance, it is becoming more and more evident that to get a rapid and cheap BCC phenotype characterization of cell populations freshly isolated from tumor samples would be of a great advantage. One could also envisage to evaluate the effect of a particular compound on a restricted set of specific genes known for their modified expression in breast cancer.

In this study, we designed a low-density microarray dedicated to breast cancer studies. It carries DNA capture sequences that are highly specific to 132 'breast' genes and 13 housekeeping genes. The 'breast' genes include many of those that have been described as differentially expressed in BCC lines, in tumors, and reported in the scientific literature before the advent of DNA microarray technology (years: ~1975-1995) (2,7). This microarray also allows gene expression analysis for candidates that are considered to play an important role in tumor cell properties such as cell proliferation, cell adhesion, proteolysis, hormone sensitivity and chemo-resistance. We used this low-density microarray to analyze gene expression profiles obtained for 11 BCC lines, including six previously well-characterized ones.

Materials and methods

Cell lines. BT-474, Hs578T, KPL-1, MCF-7, MDA-MB-231, MDA-MB-453, and T-47D BCC lines were either from American Type Culture Collection (ATCC, Rockville, MD, USA) or from Deutsche Sammlung von Mikroorganismen und Zellkulturen (DSMZ, Germany). Evsa-T cells (11) were obtained from Dr Marc Lippman. The isolation and characterization of IBEP-1, -2 and -3 BCC lines have been described previously (12-14). For more details on these 11 cell lines, please refer to Lacroix and Leclercq (2).

Cell growth studies. Cells were seeded in 96-well plates (density 2500 cells/well) in phenol red-free EMEM [Minimum Essential Medium with Earle's Balanced Salts, (Invitrogen, Carslbad, CA, USA)] supplemented with 10% inactivated dextran-coated charcoal (DCC)-stripped FCS (Invitrogen). After 24 h, cells were incubated for 24, 48 or 72 h in the same medium containing, or not, 10^{-10} M 17 ß estradiol (E_2, Sigma-Aldrich, Belgium). Cell growth was assayed by crystal violet staining as described (15).

RNA extraction. Total RNA was extracted from BCC lines with TriPure (Roche, Mannheim, Germany) according to the manufacturer's instructions. Poly(A+) RNA was obtained from total RNA using FastTrack columns (Invitrogen). RNA concentration and purity were determined by reading absorbance at 260 and 280 nm. The quality of RNA was also checked by electrophoresis on a denaturing 1% agarose gel. RNA integrity was further verified by capillary electrophoresis on the Agilent 2100 Bioanalyser (Agilent Technologies, Palo Alto, CA, USA).

Synthesis of labeled cDNA. Labeled cDNA were prepared using 0.5 μg of mRNA. Three synthetic poly(A)-tailed RNA standards prepared from Lycopersicon esculentum genes were spiked at three different amounts (10, 1 and 0.1 ng per reaction) into the purified mRNA according to the manufacturer's instructions (Eppendorf, Hamburg, Germany). These internal standards were used for quantification and estimation of experimental variation introduced during labeling and analysis. For more details concerning the cDNA preparation, please refer to de Longueville *et al* (8).

Breast cancer microarray design: 145-gene microarray. Genes represented by specific DNA capture sequences on the breast cancer microarray are listed in Table I. The table also mentions cell function or tumor property associated with the expression of each gene. In order to evaluate the reliability of the experimental hybridization, several controls of positive and negative hybridization, positive and negative detection were included on the breast cancer microarray. For normalization, 3 internal standards and 13 housekeeping genes were arrayed on the slides. The breast cancer microarray was composed of single stranded DNA probes attached to the glass support by a covalent link. Each DNA probe was present in triplicate (Fig. 1). All probes had the same length and corresponded to regions located close to the 3' end of their target mRNA (Eppendorf).

Hybridization with biotinylated-labeled cDNA. Hybridization on the breast cancer microarray was carried out according to ref.s 8 and 16. The presence of biotinylated hybrids on the microarray was detected using a fluorescent Cy3-conjugated IgG anti-biotin (Jackson ImmunoResearch Laboratories Inc., West Grove, PA, USA).

Imaging, statistical analysis and clustering. After hybridization, arrays were scanned using a confocal laser scanner (ScanArray 4000XL) (PE Applied Biosystem, Foster City, CA, USA) at a resolution of 10 μm. To maximize the dynamic range of microarrays, the same arrays were scanned using different photo-multiplier settings (PMT). The use of different intensities allows the quantification of both the high and low copy expressed genes. After image acquisition, the scanned 16-bit image was used to quantify the signal intensities with the ImaGene 5.6 software (BioDiscovery, Los Angeles, CA, USA). The fluorescent intensity of each DNA spot (average of intensity of each pixel present within the spot) was calculated using local mean background subtraction. A signal was accepted if the intensity after background subtraction was at least 2.5-fold higher than its local background. The three intensity values of the triplicate DNA spots were averaged and used to determine the intensity ratio between the reference and the test samples. Very bright element intensities (saturated signals, highly-expressed genes) were deemed unsuitable for accurate quantification because they underestimated the intensity ratios, and were excluded from further analysis.

Table I. List of genes included on the breast cancer microarray. The known function of the corresponding protein and the Genbank accession number of each cDNA are provided.

Gene symbol	Gene product name	Cell function or tumor property	Genbank #
ABCB1	Multidrug resistant 1	Transport	NM_000927
ABCC1	ATP-binding cassette, sub-family C, member 1	Transport	AJ003198
ABCG2	ATP-binding cassette, sub-family G, member 2	Transport	NM_004827
ATM	Ataxia telangiectasia mutated	Signal transduction	U26455
BAG1	BCL-2 associated athanagene	Cell surface receptor linked signal transduction	AF022224
BAK1	BCL2-antagonist/killer 1	Cell-cycle control	U16811
BAX	BCL2-associated X protein	Cell-cycle control	NM_004324
BCAR1	Breast cancer anti-estrogen resistance 1	Cell proliferation	NM_014567
BCL2	B-cell lymphoma 2	Cell-cycle control	NM_000633
BCL2L1	BCL2-like 1	Cell-cycle control	NM_001191
BECN1	Bcl-2 interacting protein beclin 1	Cell-cycle control	AF139131
BRCA1	Breast cancer 1, early onset	DNA damage response	Y08864
BRCA2	Breast cancer 2, early onset	Cytoskeleton organization and biogenesis	NM_000059
BSG	Basigin	Cell surface receptor linked signal transduction	NM_001728
CAV1	Caveolin 1	Cell structure	NM_001753
CCND1	Cyclin D1	Cell-cycle control	NM_053056
CD44	CD44 antigen	Cell adhesion	NM_000610
CDH1	Cadherin 1 (E-cadherin)	Cell adhesion	NM004360
CDH11	Cadherin 11 (OB-cadherin)	Cell adhesion	NM_001797
CDH13	Cadherin 13	Cell adhesion	U59289
CDKN1A	Cyclin-dependent kinase inhibitor 1A	Cell-cycle control	U03106
CDKN1B	Cyclin-dependent kinase inhibitor 1B	Cell-cycle control	NM_004064
CDKN1C	Cyclin-dependent kinase inhibitor 1C	Cell-cycle control	NM_000076
CDKN2A	Cyclin-dependent kinase inhibitor 2A	Cell-cycle control	L27211
CEACAM5	Carcinoembryonic antigen-related cell adhesion molecule 5	Cell adhesion	NM_004363
CSF1	Colony-stimulating factor 1	Signal transduction	M37435
CSF1R	Colony-stimulating factor 1 receptor	Signal transduction	NM_005211
CST6	Cystatin M	Proteolysis and peptidolysis	U62800
CSTA	Cystatin A	Proteolysis and peptidolysis	NM_005213
CTNNB1	Catenin, beta 1	Developmental processes	NM_001904
CTSB	Cathepsin B	Proteolysis and peptidolysis	NM_001904
CTSD	Cathepsin D	Proteolysis and peptidolysis	NM_001904
CTSL	Cathepsin L	Proteolysis and peptidolysis	NM_001912
CYP19A1	Cytochrome P450, family 19, sub-family A, polypeptide 1	Metabolism	NM_000103
ECGF1	Endothelial cell growth factor 1	Cell-cell signaling	NM_001953
EGFR	Epidermal growth factor receptor	Signal transduction	NM_005228
EIF4E	Eukaryotic translation initiation factor 4E	Protein synthesis initiation	NM_001968
EMS1	Ems1 protein (cortactin)	Protein modification	NM_005231
ERBB2	V-erb-b2 erythroblastic leukemia viral oncogene homolog 2	Signal transduction	NM_004448
ESR1	Estrogen receptor 1 (alpha)	Signal transduction	NM_000125
ESR2	Estrogen receptor 2 (beta)	Signal transduction	X99101
FGF2	Fibroblast growth factor 2	Cell-cycle control	NM_002006
Gene symbol	Gene product name	Cell function or tumor property	Genbank #
FGF8	Fibroblast growth factor 8	Cell-cycle control	U36223
FGFR1	Fibroblast growth factor receptor	Signal transduction	NM_000604
FHIT	Fragile histidine triad gene	Oncogenesis	NM_002012
FIGF	C-fos induced growth factor	Positive control of cell proliferation	NM_004469

Table I. Continued.

Gene symbol	Gene product name	Cell function or tumor property	Genbank #
FLT1	Fms-related tyrosine kinase 1	Signal transduction	NM_002019
FLT4	Fms-related tyrosine kinase 4	Signal transduction	NM_002020
GJA1	Gap junction protein, alpha 1 (connexin 43)	Cell-cell signaling	NM_000165
GJB2	Gap junction protein, beta 2 (connexin 26)	Cell-cell signaling	M86849
GSN	Gelsolin	Actin filament organization	X04412
GSTP1	Glutathione S-transferase pi	Metabolism	NM_000852
HGF	Hepatocyte growth factor	Invasive growth	X16323
IBSP	Integrin-binding sialoprotein	Tissue calcification	NM_004967
ICAM1	Intracellular adhesion molecule 1	Cell adhesion	J03132
IL11	Interleukin 11	Cell surface receptor linked signal transduction	NM_000641
IL1A	Interleukin 1 alpha	Cell surface receptor linked signal transduction	NM_000575
IL1B	Interleukin 1 beta	Cell surface receptor linked signal transduction	M15330
IL6	Interleukin 6	Cell surface receptor linked signal transduction	NM000600
IL8	Interleukin 8	Chemotaxis	NM_000584
ING1	Inhibitor of growth family, member 1	Cell-cycle control	NM_005537
ITGA6	Integrin alpha 6	Cell-cell matrix adhesion	NM_000210
ITGAV	Integrin alpha V	Cell adhesion	NM_002210
ITGB1	Integrin beta 1	Cell adhesion	NM_002211
ITGB3	Integrin beta 3	Cell adhesion	M35999
KAI1	Kangai 1	N-linked glycosylation	NM_002231
KDR	Kinase insert domain receptor	Signal transduction	NM_002253
KISS1	Kiss1 metastasis suppressor	Cytoskeleton organization and biogenesis	NM_002256
KLK3	Kallikrein 3	Proteolysis and peptidolysis	NM_001648
KRT18	Cytokeratin 18	Cytoskeleton organization and biogenesis	NM_000224
KRT19	Cytokeratin 19	Cytoskeleton organization and biogenesis	NM_002276
KRT8	Cytokeratin 8	Cytoskeleton organization and biogenesis	NM_002273
LRP	Major vault protein (lung resistance protein)	Transport	NM_017458
MDM2	Mdm2 protein	Cell-cycle control	NM_002392
MET	Hepatocyte growth factor receptor	Invasive growth	NM_0 0245
MGB1	Mammaglobin 1	Glycosylphosphatidylinositol (GPI) anchor release	NM_002411
MKI67	Ki-67	Cell-cycle control	NM_002417
MMP1	Matrix metalloproteinase 1	Proteolysis and peptidolysis	NM_002421
MMP11	Matrix metalloproteinase 11	Proteolysis and peptidolysis	NM_005940
MMP13	Matrix metalloproteinase 13	Proteolysis and peptidolysis	NM_002427
MMP14	Matrix metalloproteinase 14	Proteolysis and peptidolysis	NM_004995
MMP15	Matrix metalloproteinase 15	Proteolysis and peptidolysis	NM_002428
MMP2	Matrix metalloproteinase 2	Proteolysis and peptidolysis	NM_004530
MMP3	Matrix metalloproteinase 3	Proteolysis and peptidolysis	NM_002422
MMP7	Matrix metalloproteinase 7	Proteolysis and peptidolysis	NM_002423
MMP9	Matrix metalloproteinase 9	Proteolysis and peptidolysis	NM_004994
MUC1	Mucin 1, transmembrane	Cell adhesion	NM_002456
Gene symbol	Gene product name	Cell function or tumor property	Genbank #
MUC18	Melanoma cell adhesion molecule	Cell adhesion	NM_006500
MYC	C-myc	Transcription regulation	NM_012333

Table I. Continued.

Gene symbol	Gene product name	Cell function or tumor property	Genbank #
NCOA1	Nuclear receptor coactivator 1	Transcription	NM_003743
NCOA2	Nuclear receptor coactivator 2	Transcription	NM_006540
NCOA3	Nuclear receptor coactivator 3	Transcription	NM_006534
NCOA6	Nuclear receptor coactivator 6	Transcription	NM_014071
NCOR1	Nuclear receptor co-repressor 1	Transcription	NM_006311
NCOR2	Nuclear receptor co-repressor 2	Transcription	NM_006312
NME2	Non-metastatic cells 2	Nucleic acid metabolism	NM_002512
ODC1	Ornithine decarboxylase 1	Polyamine biosynthesis	NM_002539
PCNA	Proliferating cell nuclear antigen	DNA replication regulation	NM002592
PGR	Progesterone receptor	Signal transduction	NM_000926
PIP	Prolactin induced protein (gross cystic disease fluid protein-15)	Not defined	NM_002652
PLAT	Plasminogen activator, tissue-type	Proteolysis and peptidolysis	NM_000930
PLAU	Plasminogen activator, urokinase-type	Proteolysis and peptidolysis	NM_002658
PLAUR	Urokinase receptor	Proteolysis and peptidolysis	NM_002659
PSORS1C2	Psoriasis susceptibility 1 candidate 2	Cell-cycle control	NM_014069
PTGS2	Prostaglandin endoperoxidase synthase 2 (cyclooxygenase2)	Cell motility	NM_000963
PTHLH	Parathyroid hormone-like hormone	Cell-cell signaling	NM_002820
RB1	Retinoblastoma 1	Cell-cycle control	NM_000321
S100A4	S100 calcium-binding protein, A4	Signal transduction	NM_002961
SERPINB2	Serine (or cysteine) proteinase inhibitor, clade B, member 2	Proteolysis and peptidolysis	J02685
SERPINB5	Serine (or cysteine) proteinase inhibitor, clade B, member 5	Acute-phase response	NM_002639
SERPINE1	Serine (or cysteine) proteinase inhibitor, clade E, member 1	Proteolysis and peptidolysis	M14083
SOD2	Superoxide dismutase 2, mitochondrial	Oxidative stress response	NM_000636
SRA1	Steroid receptor RNA activator 1	Transcription	AF293024
STMN1	Stathmin 1	Cell-cycle control	NM_005563
TFF1	Trefoil factor 1 (pS2)	Cell-cycle control	NM_003225
THBS1	Thrombospondin 1	Cell adhesion	NM_003246
THBS2	Thrombospondin 2	Cell adhesion	NM_003247
TIMP1	Tissue inhibitor of metalloproteinase 1	Proteolysis and peptidolysis	NM_003254
TIMP2	Tissue inhibitor of metalloproteinase 2	Proteolysis and peptidolysis	NM_003255
TJP1	Tight junction protein 1	Intercellular junction assembly	NM_003257
TMSB10	Thymosin beta 10	Actin polymerization/depolymerization regulation	NM_021103
TNFA	Tumor necrosis factor alpha	Cell-cell signaling	NM_000594
TNFRSF11A	Tumor necrosis factor receptor superfamily, member 11A	Signal transduction	NM_003839
TNFRSF11B	Tumor necrosis factor receptor superfamily, member 11B	Signal transduction	NM_002546
TNFSF11	Tumor necrosis factor superfamily, member 11	Signal transduction	NM_003701
TOP2A	Topoisomerase (DNA) 2 alpha	DNA topological change	NM_001067
TP53	Tumor protein p53	Signal transduction	AF307851
VEGF	Vascular endothelial growth factor	Signal transduction	AF022375
VEGFB	Vascular endothelial growth factor B	Positive control of cell proliferation	U43368
VEGFC	Vascular endothelial growth factor C	Signal transduction	NM_005429
VIM	Vimentin	Cytoskeleton organization and biogenesis	NM_003380
VWF	Von Willebrand factor	Cell adhesion	NM_000552

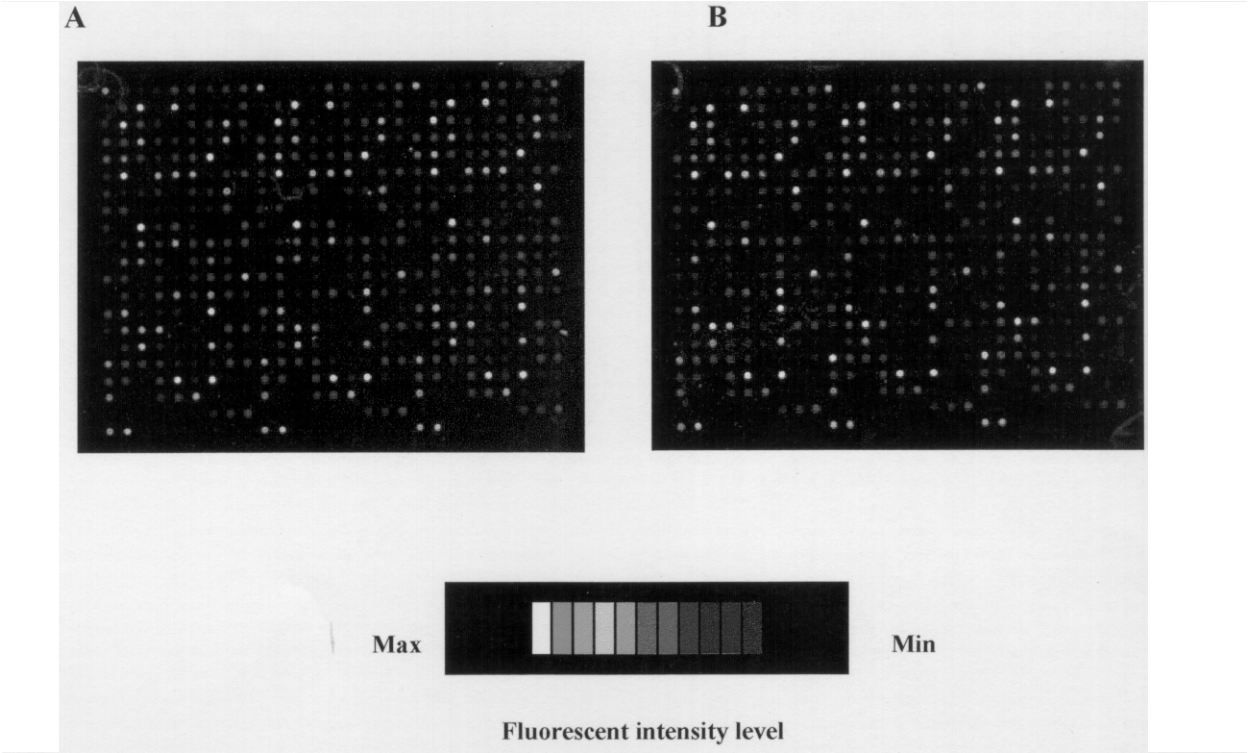

Figure 1. Breast cancer microarray hybridized with cDNA derived from mRNA extracted from a breast cancer cell line (IBEP-3) (A) or a pool of mRNAs isolated from the 11 different breast cancer cell lines (B). Fluorescence is represented in pseudo-color scale and corresponds to the expression levels of genes. Laser power of 100% and PMT gain is 70.

Several potential sources of experimental variation could occur during cDNA synthesis, labeling, hybridization and indirect detection steps. To take into account these possible variations, the data were normalized in a two-step procedure. The values were first corrected using a factor calculated from the intensity ratios of the internal standards in the reference and test samples. The microarray is divided into areas, each containing internal standards. This design allows computing of a local normalization factor for each area using the acceptable internal standard ratio of the area and evaluating the microarray homogeneity, which is taken into account in the normalization (17). However, as the internal standard control does not take into account the purity and quality of the mRNA, a second step of normalization was performed based on the expression levels of the housekeeping genes. This process involved calculating the average ratio from a subset of 13 genes previously reported as 'housekeeping' genes by abundant literature. This subset was composed of genes for which the expression level was effectively constant among the studied BCC lines.

The variance of the normalized set of housekeeping genes (except those affected by the treatment) was used to generate an estimate of expected variance, leading to a predicted confidence interval (CI) to test the significance of the ratios obtained (8,18). Ratios outside the 95% confidence interval were determined to be significantly different.

Before performing the cluster analysis, ratios falling inside the 95% confidence interval were replaced by the value 1. Clusters of hybridization profiles were created with the expression profile clustering and analysis module (http://ep.ebi.ac.uk/EP/EPCLUST) using classical agglomerative hierarchical method with the complete link. The distance computed between two hybridization profiles corresponds to the Manhattan distance (19).

Validation of relative gene expression by real-time PCR. The single strand-cDNA (ss-cDNA) was synthesized from 0.5 μg mRNA according to the RNA labeling protocol described in De Longueville *et al* (8) with the following minor modifications: i) DNAse treatment of mRNA was performed prior to cDNA synthesis; ii) the dNTP mixture contained dGTP, dATP, dTTP and dCTP each at 500 μM but no biotinylated dCTP; iii) the second addition of reverse transcriptase was omitted.

Gene specific primers corresponded to the gene sequences present on the microarray. Forward and reverse primers for real-time PCR amplification were designed with the Primer Express Software (PE Applied Biosystem).

Real-time PCR was performed on 8 genes, namely, PIP, MGB1, ESR1, PGR, GAPDH (housekeeping gene), α-Tubulin (housekeeping gene), Ribosomal Protein S9 (housekeeping gene) and RPL13A (housekeeping gene). mRNA extracted from 7 BCC lines (Evsa-T, IBEP1, IBEP2, IBEP3, MCF7, MDA-MB-231 and MDA-MB-453) was used in the real-time PCR (n=3) and each reaction was performed in triplicate.

PCR reaction mixtures contained of 12.5 μl SYBR green PCR Master Mix 2X (PE Applied Biosystems), 2.5 μl forward primer (3 mM) (PE Applied Biosystems), 2.5 μl reverse primer (3 mM) (PE Applied Biosystems), 5 μl cDNA and 2.5 μl distilled water. PCR reactions without cDNA were performed as template-free negative controls. All PCR reactions were made in duplicate with the following PCR conditions: 2 min at 50˚C, 10 min at 95˚C followed by 40 cycles of 15 sec at

95˚C and 1 min at 60˚C in 96-well optical plates (PE Applied Biosystem) in the ABI PRISM 7000 Sequence Detection System (Perkin-Elmer Life Sciences, Boston, MA, USA). The ABI PRISM 7000 Sequence Detection System Software (version 1.6) was used for data analysis according to the manufacturer's instructions (PE Applied Biosystem).

Fluorescence emission was detected for each PCR cycle and the threshold cycle (C_T) values were determined. The C_T value was defined as the actual PCR cycle when the fluorescence signal increased above the background threshold. Average C_T values from duplicate PCR reactions were normalized to average C_T values for the housekeeping gene from the same cDNA preparations. The ratio of expression of each gene in BCC lines (test samples) vs. cell line pool (reference sample) was calculated as $2^{-(\Delta\Delta CT)}$ of that condition as recommended by Perkin-Elmer where C_T is the threshold cycle and $\Delta\Delta CT$ is the difference, C_T (test gene) - C_T (housekeeping gene) for test sample minus reference sample. Values were reported as an average of triplicate analyses.

Northern-blot analysis. Total RNA (30 μg) were separated on a 0.9% agarose gel in 2.2% formaldehyde, 0.02 M 3-(N-morpholino) propane sulfonic acid (MOPS), 5 mM sodium acetate and 1 mM EDTA before transfer onto a nylon membrane (Hybond-N, Amersham, UK). Pre-hybridization, hybridization with the ^{32}P-labeled DNA probes and autoradiography were performed as described previously (20,21). The MGB1 and PIP cDNA and the 28S rRNA oligonucleotide probes were labeled using the Random Primed DNA labeling kit (Roche) according to the manufacturer's instructions. The MGB1 and PIP probes resulted from PCR amplification.

Western blot analysis. Sample preparation and blotting were performed as described previously (22). After blocking with 5% non-fat dry milk in TBS buffer containing 0.1% Tween-20 (2 h, RT), blots were incubated with D-12 anti-ERα (Santa Cruz Biotechnologies, Santa Cruz, USA) or AB-8 anti-PgR (NeoMakers, Fremont, CA, USA) and MAB1501R anti-actin (Chemicon, Temecula, CA, USA) mouse primary antibodies (respectively 1:750, 1:500 and 1:10000 dilutions, 2 h, RT). Detection was performed by chemiluminescence, using HRP-coupled goat anti-mouse secondary antibodies (Pierce, Rockford, IL, USA) (1:2000 dilution, 1.5 h, RT) and Western Pico detection system (Pierce) with a LAS-3000 imaging system (Fujifilm, Japan). Densitometric evaluations were performed using Aida Image Analyser program version 3.45.039 (Raytest, Straubenhardt, Germany) according to the manufacturer's instructions.

Results

Classification of BCC lines. Eleven BCC lines were chosen for mRNA analysis with the low-density microarray. Data obtained with each cell line was expressed with regard to a common reference, prepared by mixing equal amounts of mRNA from the 11 BCC lines. Each sample (mRNA from a cell line) was hybridized in triplicate. Each experiment was performed on a glass slide bearing two identical microarrays, one being used for the sample and the other one for the reference. Fig. 1 shows an example of data obtained with an mRNA from IBEP-3 cells (Fig. 1A) and the common reference (Fig. 1B).

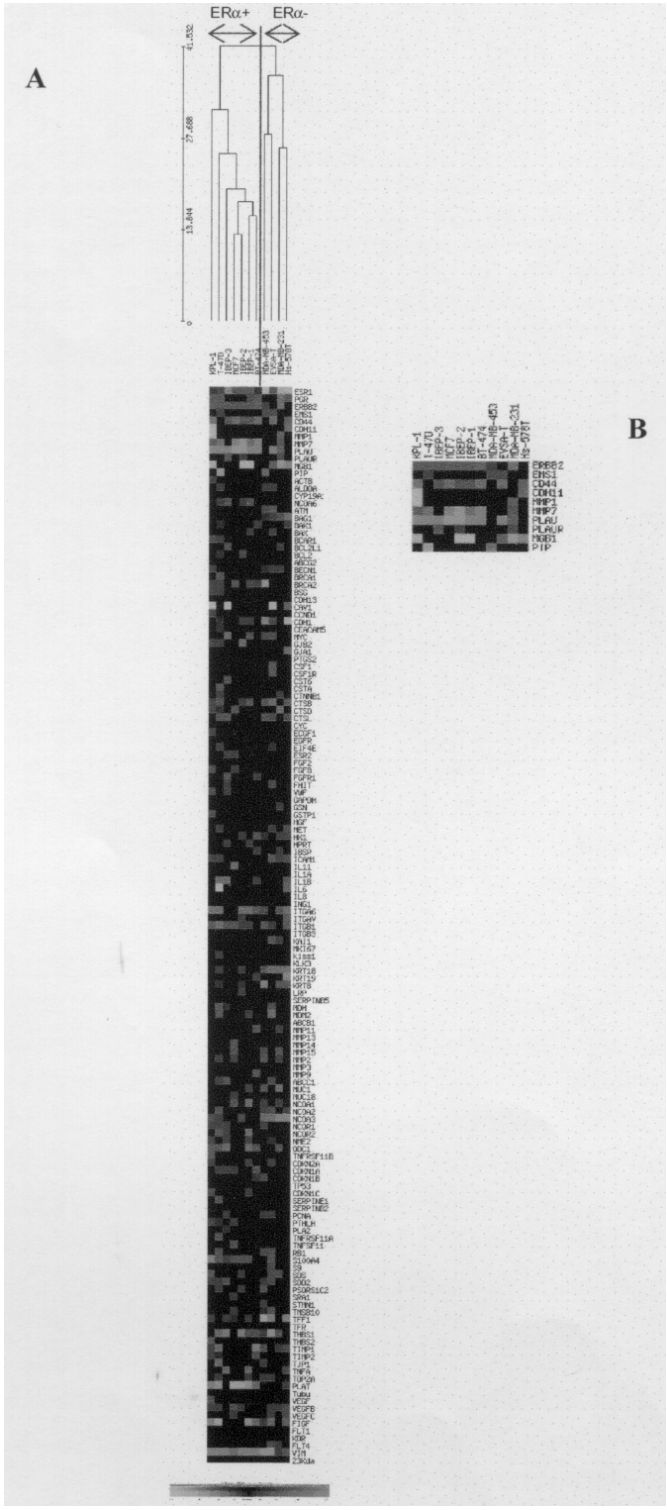

Figure 2. Hierarchical clustering analysis depicting relative gene expression differences between cell lines. (A) Complete cluster diagram that represents the 145 transcript across the 11 independent BCC lines. The red-green pseudocolor chart depicts gene expression data in comparison with cell lines. Red blocks depict genes relatively overexpressed in comparison with the measured sample whereas green blocks depict genes relatively underexpressed. The dendrogram above the color chart represents the relative similarities of the cell lines to one another. (B) High scale representation of transcripts that are expressed at high level in only one of the studied cell lines.

A

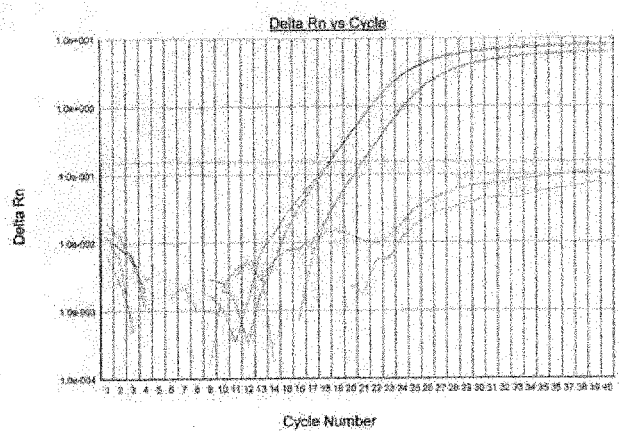

B

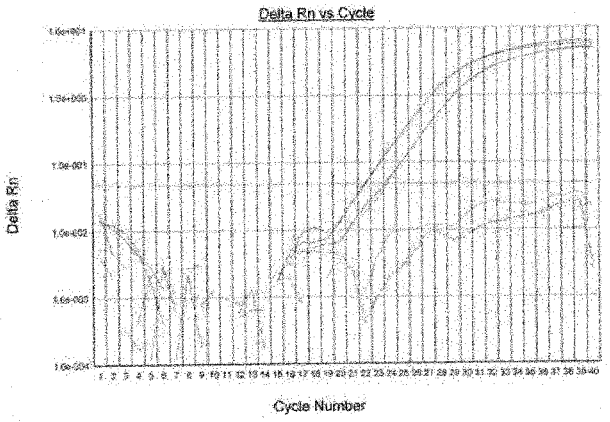

C

Gene name	Genbank #	DNA microarray	Real-Time PCR
MGB1	NM_002411	8.9	12.84
PIP	NM_002653	10.73	11.92

Figure 3. Comparison of gene expression data obtained by DNA microarray and real-time PCR. (A) Real-time PCR SYBR green I fluorescence (delta Rn) versus cycle number of *MGB1* transcript in the Evsa-T cell line and in the reference sample (pool of 11 BCC lines). (B) Real-time PCR SYBR green I fluorescence (delta Rn) versus cycle number of *PIP* transcript in the MDA-MB-453 cell line and in the reference sample (pool of 11 BCC lines). (C) Comparison of microarray and real-time PCR gene expression data. Microarray data are shown as mean ratios (BCC lines vs. reference, n=3, $p<0.05$).

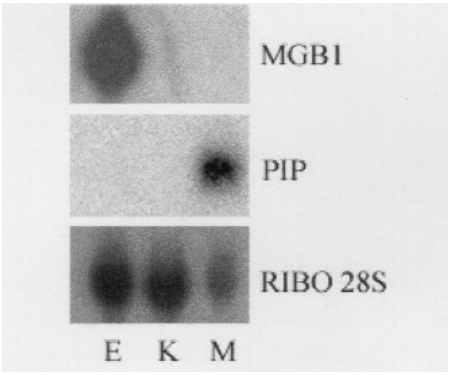

Figure 4. Northern-blot analysis of total RNA from the Evsa-T (E), KPL-1 (K) and MDA-MB-453 (M) BCC lines. The probes used were specific to *MGB1*, *PIP* or the 28S ribosomal RNA (control).

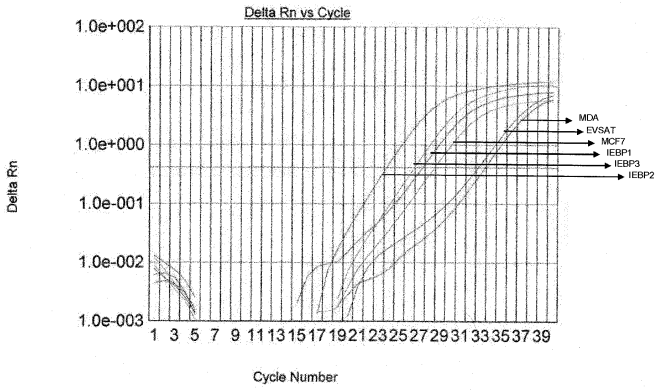

Figure 5. Real-time PCR validation of gene expression data determined by DNA microarray. Real-time PCR SYBR green I fluorescence versus cycle number of *ESR1* transcript in the Evsa-T, IBEP-1, IBEP-2, IBEP-3, MCF-7, MDA-MB-231 cell lines.

Among the 11 cell lines tested, six (BT-474, Hs578T, MCF-7, MDA-MB-231, MDA-MB-453, T-47D) had been thoroughly investigated, and expression of various markers is widely documented for these cells ('well-characterized' phenotype) making them interesting for the present study (2,23). The five other BCC lines (Evsa-T, KPL-1, IBEP-1, IBEP-2, IBEP-3) were poorly characterized.

We examined individual gene expression data obtained with the breast cancer microarray. In general, genes previously known to be associated with a 'luminal epithelial-like' BCC phenotype (*ESR1*, *PGR*, *CDH1*, *KRT8*, *KRT18*, *KRT19*, *TFF1*) were expressed at higher levels in the cell lines belonging to the ERα-positive group. In contrast, ERα-negative BCC lines (Evsa-T, Hs587T, MDA-MB-231, MDA-MB-453) had generally higher levels of mRNA specific to various markers known to be expressed in fibroblastic/mesenchymal cells. These markers included *CAV1*, *CD44*, *CDH11*, *CDH13*, *CTSB*, *CTSL*, *PTGS2*, *ICAM1*, *IL6*, *IL11*, *MMP1*, *MMP7*, *PLAU*,

PLAUR, *VIM*, etc. As shown in Fig. 2B, some genes are exclusively expressed at high level in one examined cell line. For instance, *ERBB2* was overexpressed in BT-474 and, to a less extent, in MDA-MB-453 BCC. *EMS1* expression was particularly specific to MDA-MB-453 BCC and Evsa-T. The expression level of some genes associated with the 'fibroblast-like' phenotype was particularly high in Hs578T (for *CD44* and *CDH11*) or in MDA-MB-231 (for *MMP1*, *MMP7*, *PLAU* and *PLAUR*) cells. *MGB1* and *PIP*, two genes that are specifically expressed in the mammary tissue, were also only expressed at a high level in Evsa-T and MDA-MB-453 BCC, respectively.

Microarray data were submitted to hierarchical clustering analysis, to identify systematic features in the various patterns of gene expression across the 11 BCC lines. As shown in Fig. 2, this treatment allowed a classification of the cell lines into two main dendrogram branches. Thus, data obtained with the breast cancer microarray are meaningful to discriminate between two major gene expression profiles, or 'portraits'. The first branch (left) contained the Evsa-T, Hs578T, MDA-MB-453 and MDA-MB-231 BCC lines, all of them were negative for ERα expression. In the second branch (right) were grouped the BT-474, KPL-1, IBEP-2, MCF-7 and T-47D BCC lines, which have all been described as ERα-positive, and the IBEP-1 and -3 lines. These latter were initially described as ERα-negative, based on their protein expression (14). However, we identified them as ERα-positive, at the mRNA level (see below).

Gene expression validation. Some of the data obtained with the breast cancer microarray were confirmed by RT-PCR. This was notably the case for *MGB1* and *PIP*, the genes highly expressed in Evsa-T and MDA-MD-453 BCC, respectively, and for *GAPDH* and *RPL13A*, two of the housekeeping genes.

RT-PCR data revealed that *MGB1* and *PIP* expression levels were respectively 12.84- and 11.92-fold higher in Evsa-T (Fig. 3A) and in MDA-MB453 cells (Fig. 3B). This was correlated with microarray data (respectively 8.9- and 10.13-fold-increase) (Fig. 3C). The expression level of *GADPH* and *RPL13A* was also found to be similar in all samples when analyzed with both microarray and RT-PCR techniques (data not shown).

To further confirm that the mRNA found to be over-expressed in Evsa-T and MDA-MB-453 cells were effectively specific for *MGB1* and *PIP*, we performed a Northern blot analysis on total RNA from these cell lines, as well as from the KPL-1 cells (negative control) (Fig. 4). The *MGB1* probe recognized a ~0.5-kb mRNA in Evsa-T, but not in MDA-MB-453 or in KPL-1 cells. The *PIP* probe produced a ~0.7-kb signal in MDA-MB-453 cells only. These sizes are in agreement with the data reported in the literature (24,25). Finally, an immunohistochemical study performed on Evsa-T, KPL-1, and MDA-MB-453 cells indicated the presence of the prolactin-induced protein in this latter cell line only (data not shown).

Assessment of the ERα positivity of IBEP-1 and IBEP-3 BCC. After being established in culture, IBEP-1 and IBEP-3 BCC lines have been characterized as ERα-negative, at both mRNA and protein levels (14). However, the analysis of their mRNA

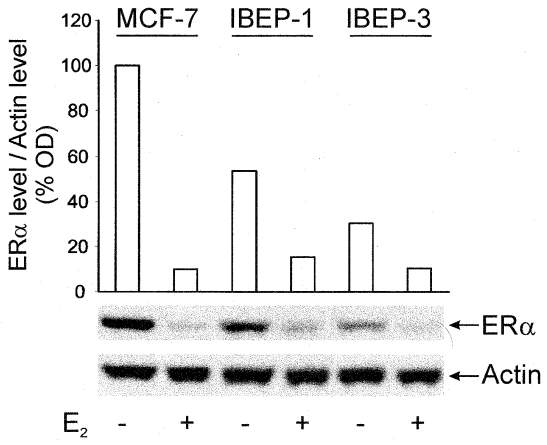

Figure 6. Influence of 10^{-10} M E_2 on cellular ERα levels in MCF-7, IBEP-1 and IBEP-3 BCC. The immunoblot is representative of two independent experiments. Results are expressed as percentages of ERα level as compared to untreated MCF-7 cells (100%).

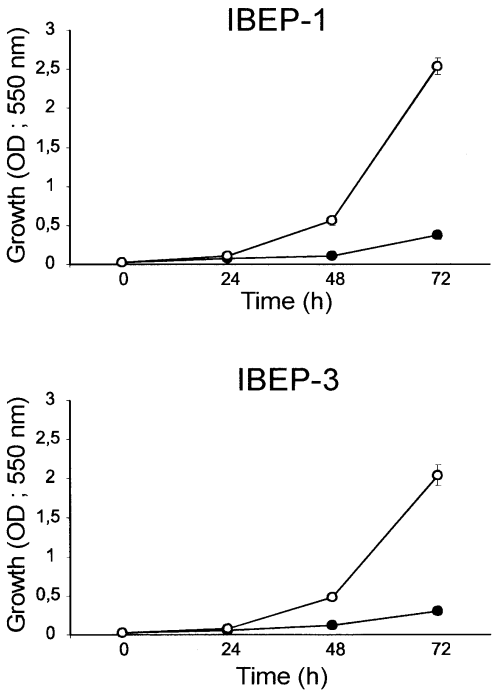

Figure 7. Influence of 10^{-10} M E_2 on IBEP-1 and IBEP-3 BCC growth. Growth was assayed by crystal violet staining and optical density (OD) was measured at 550 nm. Control, ●; E_2, ○.

by the low-density microarray classified them in the group containing the known ERα-positive BT-474, IBEP-2, KPL-1, MCF-7, T-47D cell lines (see above). We have re-examined the receptor status of these two cell lines and found that they were indeed ERα-positive and E_2-responsive.

First, RT-PCR analysis showed that the *ESR1* mRNA level in IBEP-1 and IBEP-3 BCC was close to its value in the MCF-7 and IBEP-2 cell lines (Fig. 5). This analysis also confirmed that, regarding *ESR1* expression, the Evsa-T BCC were closer to the ERα-negative MDA-MB-231 than to any of the ERα-positive cells. Second, Western blotting analysis revealed the presence of significant amounts of ERα in IBEP-1 and IBEP-3. More-

over, the receptor was down-regulated upon incubation of the cells with 10^{-10} M E_2, as also observed with MCF-7 BCC (Fig. 6). Third, cell growth studies indicated that IBEP-1 and IBEP-3 cells responded to 10^{-10} M E_2 by an increase in proliferation (Fig. 7). The proliferative effects of estrogens on BCC are essentially reported to be mediated by ERα but not ERß (26).

Discussion

A low-density microarray dedicated to the analysis of breast cancer was developed which carries 132 DNA capture probes highly specific for genes reported to have a differential expression in breast tumors and BCC lines, or to be associated with specific tumor properties (cell-cycle alteration, proteolysis, adhesion and hormone sensitivity). Using this microarray, we established the gene expression profiles of 11 BCC lines. The characteristics of six of them (BT-474, Hs578T, MCF-7, MDA-MB-231, MDA-MB-453, T-47D) have already been widely studied, notably by high-density microarray analysis (2,23,27). In consequence, these 'well-characterized' cell lines were mainly used as controls to check the quality of gene expression data obtained on the low-density microarray that we developed. The 5 other BCC lines (Evsa-T, IBEP-1, IBEP-2, IBEP-3, KPL-1) had been less characterized and were analyzed in order to obtain their 'molecular signature' based on their gene expression profile.

An important finding of previous studies, notably coming from high-density microarray analysis, is that BCC lines could be classified into 'ERα-positive/luminal epithelial-like' and 'ERα-negative/fibroblast-like' (2). From these studies, the ERα status appeared as a major molecular determinant in BCC (and tumors) classification. We assumed that these two main groups of cell lines could also be clearly distinguished by a low-density microarray, providing that the DNA sequences of the latter were selected and highly specific. The choice of the capture sequences relied mainly on the scientific literature accumulated before DNA microarray technology was developed, and it is interesting to mention that the data from the low-density microarray are generally in good agreement with data found in the literature. The data obtained for the 6 'well-characterized' cell lines were also in agreement with the 2-class sorting resulting from high-density chip analyses. On the one hand, the three ERα-positive cell lines (BT-474, MCF-7 and T-47D) and, on the other hand, the three ERα-negative lines (Hs578T, MDA-MB-231, MDA-MB-453) were clearly separated by hierarchical cluster analysis (Fig. 2). The fact that they segregated so clearly confirmed that the expression status of numerous genes is correlated (positively or negatively) to the expression of *ESR1* in BCC lines.

Of the five poorly characterized BCC lines, two were previously found to be ERα-positive: KPL-1 and IBEP-2 (2). As expected, they were classified among the three ERα-positive, 'well-characterized', MCF-7, T-47D and BT-474 cell lines. The ERα-negative Evsa-T cells (11) were effectively classified among the well-characterized ERα-negative lines (Hs578T, MDA-MB-231, MDA-MB-453) based on the microarray data. Data obtained for IBEP-1 and IBEP-3 on the low-density microarray revealed that they expressed *ESR1* mRNA, contrasting with its absence or its very low level in the well-characterized ERα-negative cells (Hs578T, MDA-MB-231, MDA-MB-453). Moreover, both IBEP-1 and IBEP-3 express progesterone receptors, which are frequently observed in ERα-positive cells and may be induced in an ERα-mediated way. Finally, IBEP-1 cells have been isolated from a patient with an ERα-positive, well-differentiated tumor, further supporting that these cells were initially misclassified as ERα-negative cells (14). We have now firmly established that IBEP-1 and IBEP-3 BCC lines are ERα-positive and express receptors at both mRNA and protein levels to similar amounts as those found in MCF-7 or IBEP-2 BCC. The reason why both IBEP cell lines were initially found to be ERα-negative is unknown. In any event, our observations underline the central place occupied by ERα in the numerous markers defining the 'luminal epithelial-like' phenotype, of which many can be analyzed with the low-density microarray.

The results obtained with the low-density microarray were generally in good agreement with data previously reported in the literature. We have pointed a series of genes that were exclusively expressed at a high level in one studied cell line. For example, we observed an overexpression of *ERBB2* in BT-474 and, to a lesser extent, in MDA-MB-453 cells as has been previously described by several investigators (28,29). In these cell lines, the overexpression results from an *ERBB2* gene amplification. The high level of *EMS1* expression in MDA-MB-453 cells is in line with data indicating that among the 11 cell lines used in this study, the *EMS1* gene is over-expressed only in these cells (30). The high level of *CD44* and *CDH11* expression in Hs578T has also been previously shown (31,32) as was the overexpression of *MMP1*, *MMP7* (33-35), *PLAU* and *PLAUR* in MDA-MB-231 cells (36,37).

The product of *MGB1*, the gene encoding mamma-globin 1, is a family member of secreted epithelial proteins. Its expression has been restricted to the mammary gland. Compared to normal breast tissue, 23% of human breast tumors were found to overexpress *MGB1* mRNA (24). This suggests the use of RT-PCR-mediated *MGB1* mRNA detection to evidence the presence of residual or metastatic cells in patients. The function of MGB1 in normal breast is unknown, but its expression in breast cancer is associated with clinical and biological features defining a less aggressive tumor phenotype (38). Regarding cell lines, a previous study reported no *MGB1* mRNA expression in MCF-7 or MDA-MB-231, while a faint signal was observed in BT-474 cells (24). Our data are in agreement with these results. In fact, among the 11 cell lines that we studied, only Evsa-T cells expressed a strikingly high *MGB1* mRNA level. These cells are, thus, interesting candidates for investigations aiming to evaluate in animal models the *in vivo* dissemination of breast cancer cells by RT-PCR, as *MGB1* is normally not expressed in non-mammary tissue.

For the first time, we show that the presence of relatively high mRNA and protein levels for *PIP* in MDA-MB-453 seems to be cell-specific as it does not occur in other BCC lines. Also known as Gross Cystic Disease Fluid Protein-15 (GCDFP-15), PIP is a 14-kDa protein that is considered as a highly specific and sensitive marker of apocrine differentiation (39) and has been used to detect breast cancer and follow breast cancer progression. PIP may be identified in most breast tumor biopsies. In cell lines, studies have revealed that besides

prolactin, various hormones and cytokines regulate PIP expression. While estrogen decreases its expression, it is maximally up-regulated by androgen (40), which is also known to increase the PRLR level in MDA-MB-453 (41). MDA-MB-453 are relatively rich in prolactin receptors (42). They have no estrogen and progesterone receptors (α), but possess a high amount of androgen receptors, which is a general characteristic of apocrine breast cells (39,43). We suggest that MDA-MB-453 BCC may serve as a pertinent model for apocrine breast cancer cells.

Microarray measurements are usually semi-quantitative, with compression of values occurring at high-fold changes (44,45). However, the data generated here by microarray were found to be very similar when compared with RT-PCR results. Furthermore, the gene expression profiles observed in this study have been confirmed for several genes by real-time PCR assays. This confirmation validates our results and supports the use of microarray technology in the breast cancer field.

In conclusion, the gene expression data generated in this study were in good agreement with the literature and real-time PCR quantification. This confirmation validates our results and supports the use of microarray technology. Despite the low number of genes studied, the gene expression patterns allowed a certain degree of classification of BCC lines. These results support the interest of a low-density microarray approach in cases where the cost and exhaustiveness of high-density microarrays may constitute a drawback. For instance, the low-density microarray could be used to obtain a rapid and inexpensive BCC phenotype evaluation in cell populations freshly isolated from tumors/clinical samples.

Acknowledgements

This work was supported by grants from the "Recherche d'Initiatives" program (Région Wallonne - Walloon Region), from the Medic Foundation and the J.C. Heuson Fund for Breast Cancer Research.

References

1. Liu ET: Classification of cancers by expression profiling. Curr Opin Genet Dev 13: 97-103, 2003.
2. Lacroix M and Leclercq G: Relevance of breast cancer cell lines as models for breast tumours: an update. Breast Cancer Res Treat 83: 249-289, 2004.
3. Cooper C: Applications of microarray technology in breast cancer research. Breast Cancer Res 3: 158-175, 2001.
4. Ross DT and Perou CM: A comparison of gene expression signatures from breast tumors and breast tissue derived cell lines. Dis Markers 17: 99-109, 2001.
5. Bertucci F, Viens P, Hingamp P, Nasser V, Houlgatte R and Birnbaum D: Breast cancer revisited using DNA array-based gene expression profiling. Int J Cancer 103: 565-571, 2003.
6. Ross DT, Scherf U, Eisen MB, Perou CM, Rees C, Spellman P, Iyer V, Jeffrey SS, van de Rijn M, Waltham M, Pergamenschikov A, Lee JC, Lashkari D, Shalon D, Myers TG, Weinstein JN, Botstein D and Brown PO: Systematic variation in gene expression patterns in human cancer cell lines. Nat Genet 24: 227-235, 2000.
7. Lacroix M, Zammatteo N, Remacle J and Leclercq G: A low-density DNA microarray for analysis of markers in breast cancer. Int J Biol Markers 17: 5-23, 2002.
8. De Longueville F, Surry D, Meneses-Lorente G, Bertholet V, Talbot V, Evrard S, Chandelier N, Pike A, Worboys P, Rasson JP, Le Bourdelles B and Remacle J: Gene expression profiling of drug metabolism and toxicology markers using a low-density DNA microarray. Biochem Pharmacol 64: 137-149, 2002.
9. Hamels S, Gala JL, Dufour S, Vannuffel P, Zammatteo N and Remacle J: Consensus PCR and microarray for diagnosis of the genus Staphylococcus, species and methicillin resistance. Biotechniques 31: 1364-1366, 1368, 1370-1372, 2001.
10. Zammatteo N, Lockman L, Brasseur F, De Plaen E, Lurquin C, Lobert PE, Hamels S, Boon T and Remacle J: DNA microarray to monitor the expression of MAGE-A genes. Clin Chem 48: 25-34, 2002.
11. Borras M, Lacroix M, Legros N and Leclercq G: Estrogen receptor-negative/progesterone receptor-positive Evsa-T mammary tumor cells: a model for assessing the biological property of this peculiar phenotype of breast cancers. Cancer Lett 120: 23-30, 1997.
12. Lacroix M, Siwek B, Marie PJ and Body JJ: Production and regulation of interleukin-11 by breast cancer cells. Cancer Lett 127: 29-35, 1998.
13. Lacroix M, Marie PJ and Body JJ: Protein production by osteoblasts: modulation by breast cancer cell-derived factors. Breast Cancer Res Treat 61: 59-67, 2000.
14. Siwek B, Larsimont D, Lacroix M and Body JJ: Establishment and characterization of three new breast-cancer cell lines. Int J Cancer 76: 677-683, 1998.
15. Lee MV, Fong EM, Singer FR and Guenette RS: Bisphosphonate treatment inhibits the growth of prostate cancer cells. Cancer Res 61: 2602-2608, 2001.
16. De Longueville F, Atienzar FA, Marcq L, Dufrane S, Evrard S, Wouters L, Leroux F, Bertholet V, Gerin B, Whomsley R, Arnould T, Remacle J and Canning M: Use of a low-density microarray for studying gene expression pattern induced by hepatotoxicants on primary cultures of rat hepatocytes. Toxicol Sci 75: 378-392, 2003.
17. Schuchhardt J, Beule D, Malik A, Wolski E, Eickhoff H, Lehrach H and Herzel H: Normalization strategies for cDNA microarrays. Nucleic Acids Res 28: E47, 2000.
18. Chen Y, Dougherty ER and Bittner ML: Ratio-based decisions and the quantitative analysis of cDNA microarray images. J Biomed Optics 2: 364-374, 1997.
19. Van Cutsem B: Classification and dissimilarity analysis. In: Lecture Notes in Statistics. Springer-Verlag (ed). 1994.
20. Lacroix M, Querton G, Hennebert P, Larsimont D and Leclercq G: Estrogen receptor analysis in primary breast tumors by ligand-binding assay, immunocytochemical assay and northern blot: a comparison. Breast Cancer Res Treat 67: 263-271, 2001.
21. Rivas A, Lacroix M, Olea-Serrano F, Laios I, Leclercq G and Olea N: Estrogenic effect of a series of bisphenol analogues on gene and protein expression in MCF-7 breast cancer cells. J Steroid Biochem Mol Biol 82: 45-53, 2002.
22. Journe F, Body JJ, Leclercq G, Nonclercq D and Laurent G: Estrogen responsiveness of IBEP-2, a new human cell line derived from breast carcinoma. Breast Cancer Res Treat 86: 39-53, 2004.
23. Sommers CL, Byers SW, Thompson EW, Torri JA and Gelmann EP: Differentiation state and invasiveness of human breast cancer cell lines. Breast Cancer Res Treat 31: 325-335, 1994.
24. Watson MA and Fleming TP: Mammaglobin, a mammary-specific member of the uteroglobin gene family, is overexpressed in human breast cancer. Cancer Res 56: 860-865, 1996.
25. Murphy LC, Tsuyuki D, Myal Y and Shiu RP: Isolation and sequencing of a cDNA clone for a prolactin-inducible protein (PIP). Regulation of PIP gene expression in the human breast cancer cell line, T-47D. J Biol Chem 262: 15236-15241, 1987.
26. Dowsett M and Ashworth A: New biology of the oestrogen receptor. Lancet 362: 260-262, 2003.
27. Perou CM, Jeffrey SS, van de Rijn M, Rees CA, Eisen MB, Ross DT, Pergamenschikov A, Williams CF, Zhu SX, Lee JC, Lashkari D, Shalon D, Brown PO and Botstein D: Distinctive gene expression patterns in human mammary epithelial cells and breast cancers. Proc Natl Acad Sci USA 96: 9212-9217, 1999.
28. Jarvinen TA, Tanner M, Rantanen V, Barlund M, Borg A, Grenman S and Isola J: Amplification and deletion of topoisomerase IIalpha associate with ErbB-2 amplification and affect sensitivity to topoisomerase II inhibitor doxorubicin in breast cancer. Am J Pathol 156: 839-847, 2000.
29. Kauraniemi P, Barlund M, Monni O and Kallioniemi A: New amplified and highly expressed genes discovered in the ERBB2 amplicon in breast cancer by cDNA microarrays. Cancer Res 61: 8235-8240, 2001.
30. Campbell DH, De Fazio A, Sutherland RL and Daly RJ: Expression and tyrosine phosphorylation of EMS1 in human breast cancer cell lines. Int J Cancer 68: 485-492, 1996.

31. Culty M, Shizari M, Thompson EW and Underhill CB: Binding and degradation of hyaluronan by human breast cancer cell lines expressing different forms of CD44: correlation with invasive potential. J Cell Physiol 160: 275-286, 1994.
32. Pishvaian MJ, Feltes CM, Thompson P, Bussemakers MJ, Schalken JA and Byers SW: Cadherin-11 is expressed in invasive breast cancer cell lines. Cancer Res 59: 947-952, 1999.
33. Bachmeier BE, Nerlich AG, Lichtinghagen R and Sommerhoff CP: Matrix metalloproteinases (MMPs) in breast cancer cell lines of different tumorigenicity. Anticancer Res 21: 3821-3828, 2001.
34. Balduyck M, Zerimech F, Gouyer V, Lemaire R, Hemon B, Grard G, Thiebaut C, Lemaire V, Dacquembronne E, Duhem T, Lebrun A, Dejonghe MJ and Huet G: Specific expression of matrix metalloproteinases 1, 3, 9 and 13 associated with invasiveness of breast cancer cells *in vitro*. Clin Exp Metastasis 18: 171-178, 2000.
35. Giambernardi TA, Grant GM, Taylor GP, Hay RJ, Maher VM, McCormick JJ and Klebe RJ: Overview of matrix metalloproteinase expression in cultured human cells. Matrix Biol 16: 483-496, 1998.
36. Holst-Hansen C, Johannessen B, Hoyer-Hansen G, Romer J, Ellis V and Brunner N: Urokinase-type plasminogen activation in three human breast cancer cell lines correlates with their *in vitro* invasiveness. Clin Exp Metastasis 14: 297-307, 1996.
37. Mangel WF, Toledo DL, Nardulli AM, Reiner GC, Norman MJ and Katzenellenbogen BS: Plasminogen activators in human breast cancer cell lines: hormonal regulation and properties. J Steroid Biochem 30: 79-88, 1988.
38. Nunez-Villar MJ, Martinez-Arribas F, Pollan M, Lucas AR, Sanchez J, Tejerina A and Schneider J: Elevated mammaglobin (h-MAM) expression in breast cancer is associated with clinical and biological features defining a less aggressive tumour phenotype. Breast Cancer Res 5: R65-R70, 2003.
39. Jones C, Damiani S, Wells D, Chaggar R, Lakhani SR and Eusebi V: Molecular cytogenetic comparison of apocrine hyperplasia and apocrine carcinoma of the breast. Am J Pathol 158: 207-214, 2001.
40. Myal Y, Iwasiow B, Cosby H, Yarmill A, Blanchard A, Tsuyuki D, Fresnoza A, Duckworth ML and Shiu RP: Analysis of tissue- and hormone-specific regulation of the human prolactin-inducible protein/gross cystic disease fluid protein-15 gene in transgenic mice. J Mol Endocrinol 21: 217-223, 1998.
41. Ormandy CJ, Clarke CL, Kelly PA and Sutherland RL: Androgen regulation of prolactin-receptor gene expression in MCF-7 and MDA-MB-453 human breast cancer cells. Int J Cancer 50: 777-782, 1992.
42. Peirce SK and Chen WY: Quantification of prolactin receptor mRNA in multiple human tissues and cancer cell lines by real-time RT-PCR. J Endocrinol 171: R1-R4, 2001
43. Hall RE, Birrell SN, Tilley WD and Sutherland RL: MDA-MB-453, an androgen-responsive human breast carcinoma cell line with high level androgen receptor expression. Eur J Cancer 30A: 484-490, 1994.
44. Yuen T, Zhang W, Ebersole BJ and Sealfon SC: Monitoring G-protein-coupled receptor signaling with DNA microarrays and real-time polymerase chain reaction. Methods Enzymol 345: 556-569, 2002.
45. Gerhold D, Lu M, Xu J, Austin C, Caskey CT and Rushmore T: Monitoring expression of genes involved in drug metabolism and toxicology using DNA microarrays. Physiol Genomics 5: 161-170, 2001.